

Assessing Spatio-temporal Characteristics of Water Storage Changes in the Mountainous Areas of Central Asia Based on GRACE

ZHANG Pengfei^{1,2}, CHEN Xi¹, BAO Anming¹, LIU Tie¹, Felix NDAYISABA^{1,2}

(1. Xinjiang Institute of Ecology and Geography, Chinese Academy of Sciences, Ürümqi 830011, China; 2. University of Chinese Academy of Sciences, Beijing 100049, China)

Abstract: The mountainous areas of Central Asia provide substantial water resources, and studying change in water storage and the impacts of precipitation and snow cover in the mountain ranges of Central Asia is of the greatest importance for understanding regional water shortages and the main factors. Data from the GRACE (Gravity Recovery and Climate Experiment) satellites, precipitation products and snow-covered area data were used to analyze the spatio-temporal characteristics of water storage changes and the effects of precipitation and snow cover from April 2002 to December 2013. The results were computed for each mountain ranges, and the following conclusions were drawn. The water storage in the mountainous areas of Central Asia as a whole increases in summer and winter, whereas it decreases in autumn. The water storage is affected by precipitation to some extent and some areas exhibit hysteresis. The area of positive water storage changes moves from west to east over the course of the year. The water storage declined during the period 2002–2004. It then returned to a higher level in 2005–2006 and featured lower levels in 2007–2009. Subsequently, the water storage increased gradually from 2010 to 2013. The Eastern Tianshan Mountains and Western Tianshan Mountain subzones examined in this study display similar tendencies, and the trends observed in the Karakorum Mountains and the Kunlun Mountains are also similar. However, the Eastern Tianshan Mountains and Western Tianshan Mountains were influenced by precipitation to a greater degree than the latter two ranges. The water storage in Qilian Mountains showed a pronounced increasing trend, and this range is the most strongly affected by precipitation. Based on an analysis of all investigated subzones, precipitation has the greatest influence on total water storage relative to the snow covered area in some areas of Central Asia. The results obtained from this study will be of value for scientists studying the mechanisms that influence changes in water storage in Central Asia.

Keywords: water storage; Gravity Recovery and Climate Experiment (GRACE); mountainous areas; Central Asia; precipitation

Citation: Zhang Pengfei, Chen Xi, Bao Anming, Liu Tie, Ndayisaba Felix, 2017. Assessing spatio-temporal characteristics of water storage changes in the mountainous areas of Central Asia based on GRACE. *Chinese Geographical Science*, 27(6): 918–933. doi: 10.1007/s11769-017-0914-6

1 Introduction

Glaciers and snowpack are the two major water sources in Central Asia (Shi *et al.*, 2002). Water resources originating from ice and snow in high mountains are the lifeblood of oases in arid regions (Wang *et al.*, 2014). An understanding of dynamic changes in water resources is needed to assess those resources in Central Asia, espe-

cially in the mountains, where water is scarce. As shown by many datasets, climatic variations have important effects on Central Asia's natural environment (Baker *et al.*, 2000). Central Asia is in the hinterland of the Eurasian continent. It experiences an extremely dry climate that features limited rainfall and strong evaporation. The temperature fluctuations are also large in this area (Yu *et al.*, 2006). The high-altitude mountains in Central Asia

Received date: 2017-01-09; accepted date: 2017-05-04

Foundation item: Under the auspices of National Natural Science Foundation of China (No. 41371419), Key Program for International Science and Technique Cooperation Projects of China (No. 2010DFA92720-04)

Corresponding author: BAO Anming. E-mail: baoam@ms.xjb.ac.cn

© Science Press, Northeast Institute of Geography and Agroecology, CAS and Springer-Verlag Berlin Heidelberg 2017

have substantial rain shadows. Thus, the water resources in the mountainous areas of Central Asia nurture societies and oases in Central Asia. Almost all of the rainfall falling in the mountains and the melt-water from snow flows to the oases located downstream. Therefore, the usable water resources in the oases depend on the amount of precipitation falling in the mountains. Unfortunately, observations of precipitation in these mountainous areas are scarce, and many regions presently lack data. In the mountainous areas of Central Asia, the main causes of changes in the gravity field are precipitation and the temporal and spatial characteristics of glaciers in different seasons (Wahr *et al.*, 1998). But the traditional methods for assessing water storage have some certain limitations. Interpreting satellite acquired remote sensing data to estimate soil water. Such estimates are confined to the upper few centimeters of the soil column. Monitoring surface water and ground water using weather stations and hydrometric stations. This method is less accurate in estimating water storage, and it is difficult to extend to larger scales. Combining meteorological data and hydrological data and physical laws to determine water storage. The Global Land Data Assimilation (GLDAS) is one example of this approach. However, the result is not deterministic in ungauged regions (Tapley *et al.*, 2004). The inversion of satellite gravity data, such as those from the GRACE (Gravity Recovery and Climate Experiment) satellites, to estimate water storage is yielding unprecedented amounts of information on regional water storage, especially the depth to water (Rodell and Famiglietti, 2001). Through accurate monitoring of the changes in Earth's gravity field over time, information on cases in which water storage is changing can be acquired (Güntner, 2008). Monitoring changes in the gravitational field of the Earth to assess changes in total water storage is helpful for estimating the water resources in mountainous regions by obtaining the gravity field of the Earth. Water storage in mountainous areas is affected by precipitation, evaporation, and other hydrologic processes, but precipitation represents the only input to the water resource. By analyzing changes in water storage and precipitation characteristics over time, a relationship between these two variables can be found. It is helpful to learn more about the details of the hydrologic cycle within the study area.

GRACE has been used to estimate water storage for

approximately 10 years. In a collaborative effort before 2002, when the GRACE data began to be collected, Swenson and Wahr (2002) noted the necessity of developing a method of optimizing the data. This effort laid the foundation for GRACE time-variable gravity processing and research. With the development of new algorithms and increased accuracy, studies involving GRACE have focused on large watersheds such as the Amazon-Orinoco (Tapley *et al.*, 2004; Wahr *et al.*, 2004), the Mississippi-Ohio (Swenson *et al.*, 2003), the Yangtze River Basin (Zhang *et al.*, 2015), the Heihe River Basin (Zhang *et al.*, 2004), and parts of southwestern China (Rodell *et al.*, 2004), to mention just a few. In particular, Hu *et al.* (2006) noted large seasonal changes in water storage within the Yangtze River Basin. They were able to distinguish an annual change in water storage within the Yangtze River Basin of approximately 3.40 cm water equivalent thickness. This study considered only the accuracy of the data and variations in water storage; the factors driving these changes were not examined. Rodell *et al.* (2009) incorporated 73 months of GRACE data processed by the Center for Space Research (CSR) into the GLDAS modelled soil-water fields and concluded that the region lost 109 km³ of groundwater between August 2002 and October 2008 as a consequence of irrigation withdrawals. However, this study is based on the assumption that groundwater sharply reduced, leading to a change in total water storage, and the results can be used only in the specific study area. Using the GRACE GFZ RL04 dataset to study 27 rivers basins that the Amazon, Lena and Mackenzie Rivers had experienced increases in interannual variations in water storage, whereas the Congo, Mississippi, Ganges, Yukon and Yarlung Zangbo Rivers reflected the opposite conclusion (Yamamoto *et al.*, 2007). However, the areas examined in these studies are all very large river basins; so far, little attention has been paid to mountainous areas. Due to the limited resolution of GRACE, it can be used for only large-scale regions, although the water storage changes derived from GRACE can show the main trends in smaller areas.

Taken together, most of the studies involving GRACE have focused on the contributing areas, and it has been difficult to assess various elements of the hydrological budget given that almost all of rivers and lakes in Central Asia are far inland. In addition, few scientists have used GRACE data to study total terres-

trial water storage in Central Asia, especially mountainous Central Asia, many research results indicate that it is possible to study mountainous Central Asia using GRACE data, and the precision of estimates of water storage changes is also promising.

This study uses a long time series of GRACE data (April 2002 to December 2013) together with contemporaneous precipitation data, to analyze tendencies in the annual-scale temporal and spatial variations in water storage within the mountainous regions of Central Asia and identify consistent trends between water storage and precipitation in the region, and to determine the relation between precipitation and water storage. By studying the tendencies of total water storage and the influences of precipitation and snow cover on water storage in Central Asia, resource allocation based on scientific facts can be determined for Central Asia.

2 Materials and Methods

2.1 Study area

The study area was established by combining Central Asia with the boundaries of its surrounding mountainous regions. In addition, based on the GTOPO30 DTM (Digital Terrain Model) topographic data covering Central Asia and related definitions of the mountainous regions, the study area was divided into six parts, namely the Altay Mountains, the Eastern Tianshan Mountains, the Western Tianshan Mountains, the Karakorum Mountains, the Kunlun Mountains and the Qilian Mountains (Fig. 1). The mountains in Central Asia are high in the northwest and low in the southeast,

and they contain most of the spectacular mountainous areas in Asia. More than 4000 glaciers cover the summit areas of these mountains, and the total area of these glaciers is more than 11 000 km² (Chen *et al*, 2006). The largest glacier is approximately 71 km long and has 33 tributaries; the total area of this glacier complex is 900 km². As a consequence of Central Asia's location within the Eurasia hinterland, the mountains to the southeast cut off the warm wet air currents from the Indian Ocean and the Pacific Ocean. The study area is dominated by a temperate continental climate. It is characterized by low precipitation, high temperature and high evaporation. The smallest of the six subzones is the Eastern Tianshan Mountains, which has an area of 4.30×10^4 km². As is shown in the study of the central Tianshan Mountains (Sun *et al*, 2016), the area of the northern slope of the Tianshan Mountains is 1.15×10^5 km², and the area of the southern slope is 1.78×10^5 km². It has been shown that the water estimates from GRACE have good precision in the central portion of the Tianshan Mountains. This high precision means that GRACE gravity field solutions can be used to analyze water storage in the Tianshan Mountains and the GRACE gravity field solutions can also be used to analyze total water storage in the six subzones.

2.2 Datasets

The data used in this study consist of 130 months of GRACE time-variable gravity data covering the period from April 2002 to December 2013 that were obtained from the CSR (Center for Space Research) at the University of Texas at Austin. Missing data were not

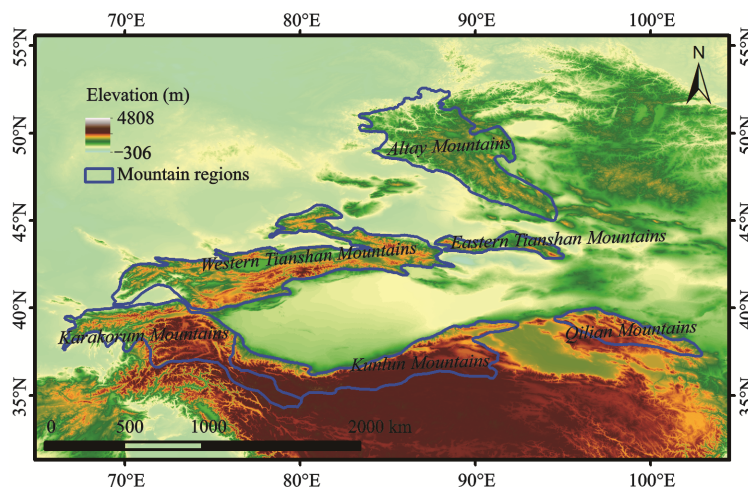


Fig. 1 Location of study area

interpolated, in order to avoid affecting the analytical results. Precipitation products and snow products covering the same region and period were also used.

2.2.1 Gravity Recovery and Climate Experiment (GRACE)

The twin GRACE satellites were launched in March 2002 by the National Aeronautics and Space Administration (NASA) and the German Aerospace Center (DLR, Deutsches Zentrum für Luft- und Raumfahrt e.V.). Their temporal resolution is approximately 30 days. At present, the main institutions that publish the GRACE data are CSR at the University of Texas at Austin (<http://www.csr.utexas.edu/grace>), the German Research Centre for Geosciences (GFZ, <http://isdc.gfz-potsdam.de/grace>) and the Jet Propulsion Laboratory (JPL, <http://podaac.jpl.nasa.gov/grace>). This study employs the dataset provided by CSR. The Level-2 release (RL05) gravity field solutions published by CSR consist of a set of fully normalized spherical harmonic coefficients of the geopotential up to 0.25° and order 60, and the spatial resolution of this data product is 1° × 1° (Lemoine *et al.*, 2007). As has been shown in several studies of GRACE gravity field solutions, the differences among the products from different processing centres are very small (Seyoum and Milewski, 2016), and the CSR processing leads to stronger agreement between the hydrological signal and the residual values. Moreover, the GRACE data with CSR processing have been widely used in studying water storage changes (Nastula *et al.*, 2015).

2.2.2 Precipitation products

The precipitation product, which contains monthly values of surface precipitation on a 0.5° × 0.5° grid, was downloaded from the China Meteorological Data Sharing Centre (CMDC, <http://data.cma.cn/>). The temporal resolution is one month and the spatial resolution is 0.5° × 0.5°. This dataset covers a range of longitudes of 72°E–136°E and a latitudes of 18°N–54°N.

2.2.3 MODIS snow products

The MOD10A2 product is used to calculate the snow cover within the different subzones. The dataset was obtained from NASA (<https://earthdata.nasa.gov>). The spatial resolution of this dataset is 500 m, and its temporal resolution is 8 days. The product has been produced using data collected at many different times; thus, the effects of clouds have been substantially reduced.

2.3 Methodology

Changes in the Earth’s gravity field are mainly caused

by the three states of water, which include solid water, liquid water and water vapour. The gravity field is also influenced by other geophysical processes, including postglacial rebound and seismic deformation (Crowley *et al.*, 2008). The information on the gravitational field measured by GRACE primarily indicates changes in the Earth’s gravity field, which can be used to estimate changes in water storage. The generic method of handling was used to obtain the water storage products (Andersen and Hindere, 2005).

To provide a better understanding of the degree of variation, the standard deviations of water storage within the six subzones are calculated using Equation (1).

$$S = \sqrt{\frac{\sum_{i=1}^n (S_i - \bar{S})^2}{n}} \tag{1}$$

where S represents the standard deviation of the six subzones during the reference months, S_i is the equivalent water thickness (EWT) of subzone i during the reference months from 2003 to 2013, \bar{S} is the average value of the six subzones during the reference months from 2003 to 2013, and n is 11. To assess the correlations between precipitation, ice cover and total water storage and thus to compare the incidence of precipitation and ice cover to total water storage, Pearson’s correlation coefficient is calculated using Equation (2).

$$r_{xy} = \frac{\sum_{i=1}^n (x_i - \bar{x})(y_i - \bar{y})}{\sqrt{\sum_{i=1}^n (x_i - \bar{x})^2 \sum_{i=1}^n (y_i - \bar{y})^2}} \tag{2}$$

where n represents the sample size, \bar{x} represents the mean value of variable x , and \bar{y} is the mean value of variable y . When r_{xy} is positive, x and y are positively correlated. When r_{xy} is negative, x and y are negatively correlated. If $r = \pm 1$, x and y display a one-to-one correspondence. As $|r|$ increases, the relationship between x and y becomes stronger.

3 Results

3.1 Temporal and spatial variations in total water storage

Data representing equivalent water thickness (EWT)

over time in the six subzones representing different mountain ranges (the Altay Mountains, the Eastern Tianshan Mountains, the Western Tianshan Mountains, the Karakorum Mountains, the Kunlun Mountains and the Qilian Mountains) were obtained, from which the overall changes in the equivalent water thickness can be assessed. The total equivalent water thickness changes in the six subzones from April 2002 to December 2013 were estimated to understand the spatial and temporal variations in the EWT data.

3.1.1 Variation of water storage in different mountain ranges

To better understand the monthly variations in EWT changes among the subzones, February, April, July and November are chosen as representative months to describe the characteristics of the corresponding seasons (Fig. 2), based on the data integrity and the corresponding season of the four representative months.

Within the Altay Mountains, the EWT changes increase rapidly in the northwest and increase slowly in the southeast in February and April, whereas they increase in the south and decrease in the north in July and November in most years. Within the Western Tianshan Mountains, the EWT changes increase in the northwest and decrease in the southeast during February, April and July. On the other hand, the opposite pattern was observed in November. The EWT changes within the Eastern Tianshan Mountains display no significant changes. Within the Karakorum Mountains, the Kunlun Mountains and the Qilian Mountains, the EWT changes increase in the west and decrease in the east during February and April. Meanwhile, the EWT changes within these ranges display the opposite pattern in July and November. Although the EWT changes are mainly influenced by climatic factors and human activities, the EWT changes in the mountainous areas of Central Asia are hardly affected by human activities and are mainly influenced by climatic factors.

In terms of their temporal evolution, the EWT changes within some of the mountain ranges fluctuate smoothly, but the different subzones display different values in different months (Fig. 3).

Most of the points representing the EWT changes in April are above zero, except for those representing the Qilian Mountains. On the other hand, most of the points reflect values less than zero in November. Moreover, the EWT changes fluctuate around zero in most of the sub-

zones, except for the Qilian Mountains in February, and the EWT changes are positive in July during most of the years studied, except in the Altay Mountains. Moreover, Fig. 3 provides further evidence that the changes show a bimodal trend in the Tianshan, the Western Tianshan Mountains, the Karakorum Mountains and the Kunlun Mountains because the precipitation varies seasonally. The amplitude of changes in the Altay Mountains increases over time, except in November; the amplitude of changes in the Western Tianshan Mountains increases over time in February and November, whereas it increases and then decreases in April and July; the amplitude of changes in the Eastern Tianshan Mountains decreases over time, except in July; the amplitude of changes in the Karakorum Mountains and the Kunlun Mountains decrease over time; and the amplitude of changes in the Qilian Mountains remains essentially the same over time.

Table 1 shows that the largest standard deviation of the six subzones in February is that of the Kunlun Mountains, and the smallest standard deviation is that of the Eastern Tianshan Mountains. On the other hand, the largest degrees of dispersion of the EWT changes of the six subzones are those of the Karakorum Mountains in April, July and November, and the smallest degrees of dispersion of the EWT changes are those of the Eastern Tianshan Mountains in April, July and November.

2006 is chosen as a representative year to understand the annual variance of the EWT changes (Fig. 4). Based on Fig. 4, EWT changes over almost the whole study area reflect strong increases, especially in the central Tianshan Mountains and the Altay Mountains, whereas the increase reflected by the EWT changes within the Qilian Mountains is less. From February to May, the spatial variations in the EWT changes are similar and reflect positive values in the north and west and negative values in the south and east. The largest areas of positive values are the western part of the Western Tianshan Mountains and the western part of the Karakorum Mountains, whereas the largest areas of negative values are the eastern part of the Kunlun Mountains and the Qilian Mountains. In July, the whole study area shows a modest increase. From August to December, the spatial distribution of EWT changes shows the opposite of the spatial distribution observed in February to May. Hence, these maps of the EWT changes during a single year show that the area with positive values moves from west to east.

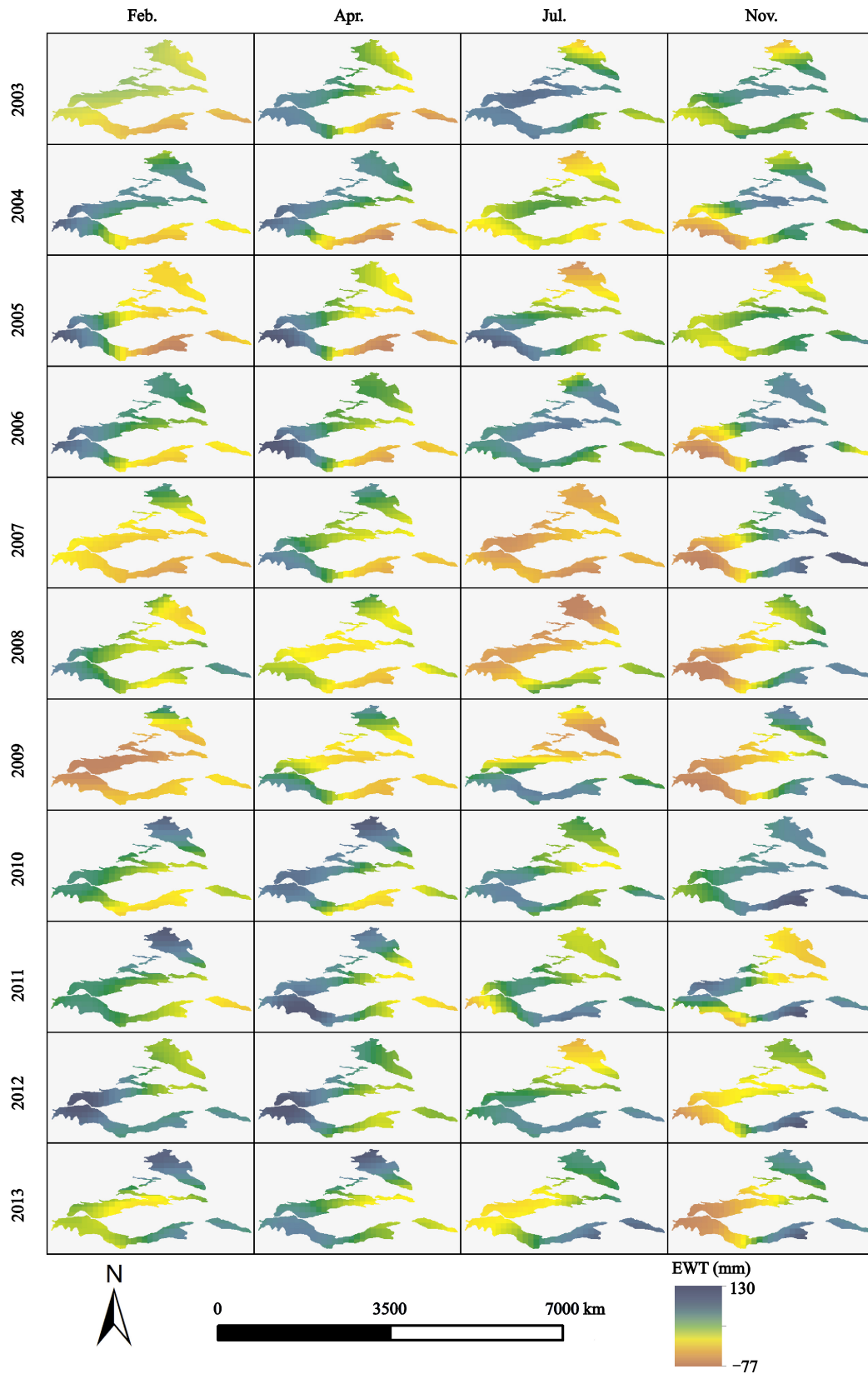


Fig. 2 Spatial distributions of equivalent water thickness (EWT) changes during the representative months. The data for 2002 are missing; mountains' information are shown in Fig. 1

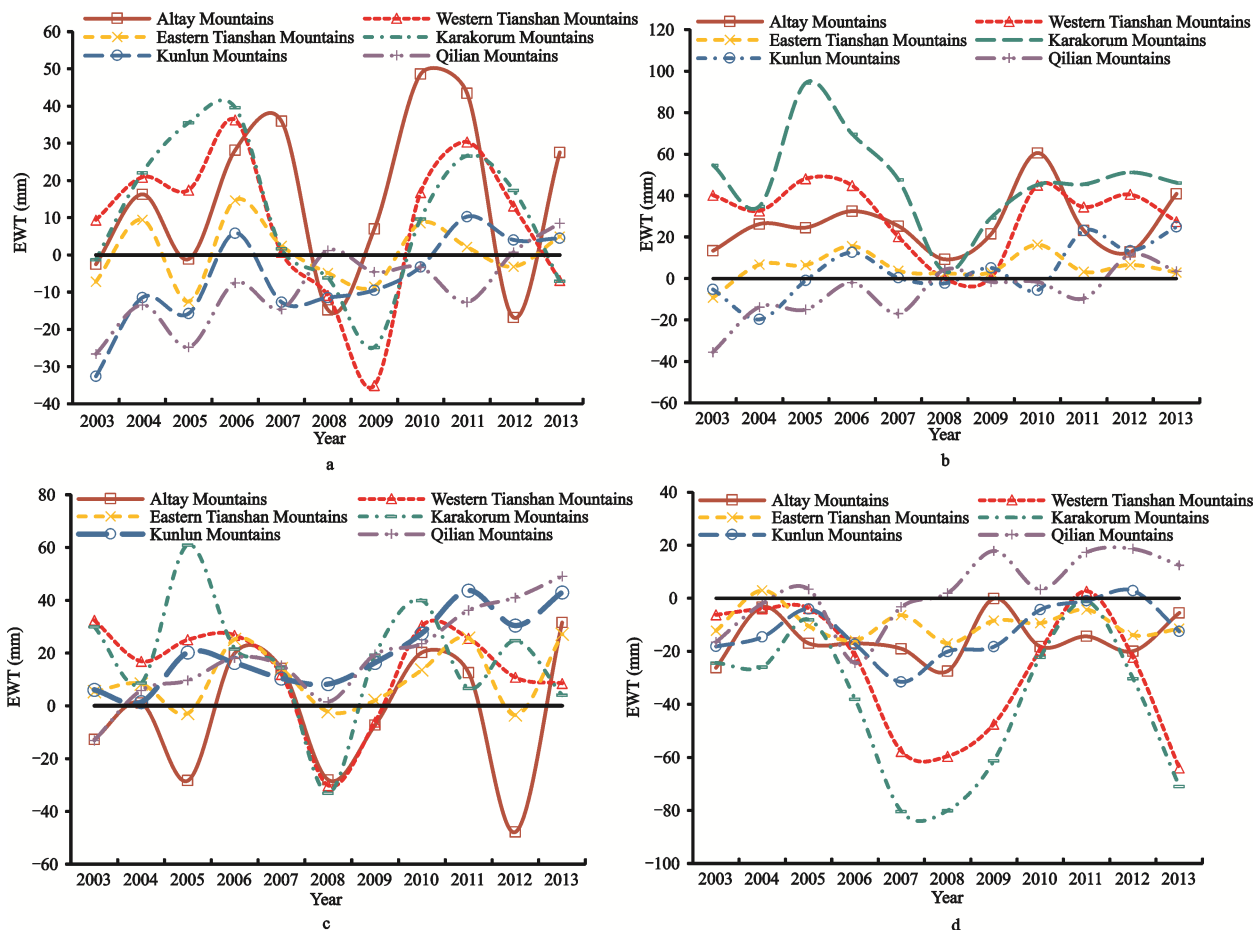


Fig. 3 Comparisons of the equivalent water thickness (EWT) changes in the subzones during the characteristic months (a. February; b. April; c. July; d. November)

Table 1 Standard deviations associated with the six subzones during the characteristic months

	Altay Mountains	Western Tianshan Mountains	Eastern Tianshan Mountains	Karakorum Mountains	Kunlun Mountain	Qilian Mountains
February	21.81	19.41	8.10	18.98	111.82	10.37
April	13.82	16.23	6.51	21.74	12.72	12.35
July	23.73	17.67	11.20	22.47	13.64	17.37
November	8.45	23.87	5.40	27.00	9.61	13.33

The monthly average EWT changes for the six subzones were calculated (Fig. 5) to enable better understanding of the variations within these subzones. The EWT changes in these three mountain ranges increase from January to April, when they reach their maximum values, and then decline to their minimum values in September or October. A modest increase occurs subsequently. Furthermore, the Kunlun Mountains and the Qilian Mountains display similar trends. The EWT changes within these two ranges increase from January to July and then decline until the end of the year. On the other hand, the Eastern Tianshan

Mountains displays reduced variability. In regard to the degree of dispersion of monthly mean values of water storage changes, the Karakorum Mountains has the largest value of the six subzones, which is 32.99. The Eastern Tianshan Mountains has the smallest value, which is 6.91.

3.1.2 Yearly variations in water storage changes in the different mountains ranges

To analyze the details of the water storage changes, the temporal variations in each mountain range are investigated. Fig. 6 presents the temporal variations in water storage changes within the six subzones.

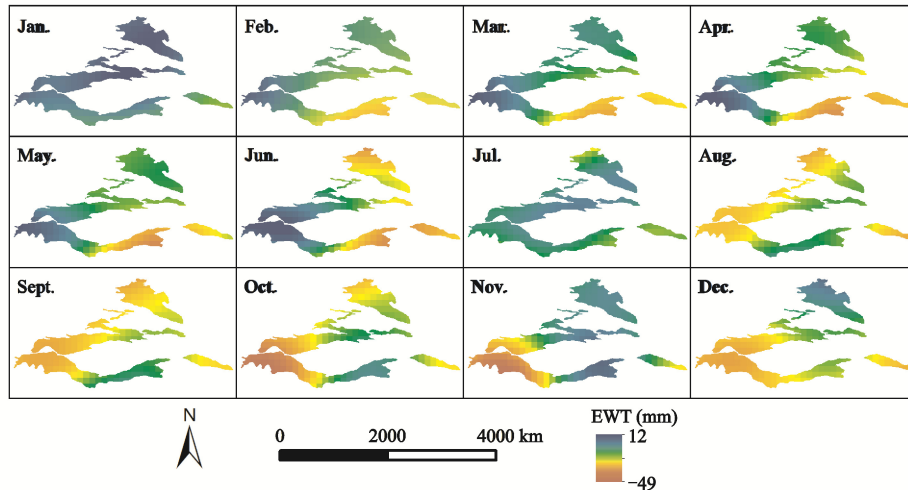


Fig. 4 Equivalent water thickness (EWT) in different months of 2006. Mountains' information shown in Fig. 1

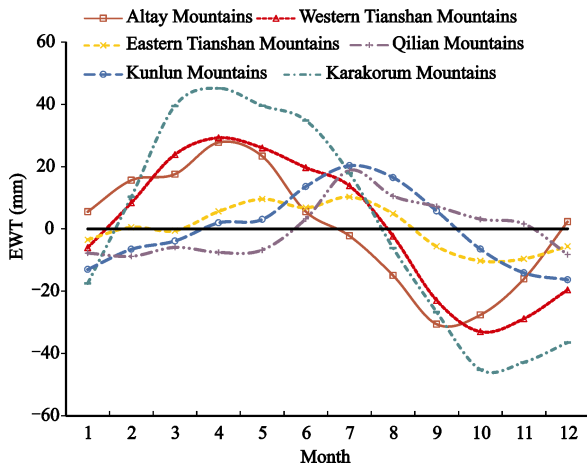


Fig. 5 Comparisons of monthly average equivalent water thickness (EWT) changes among the subzones

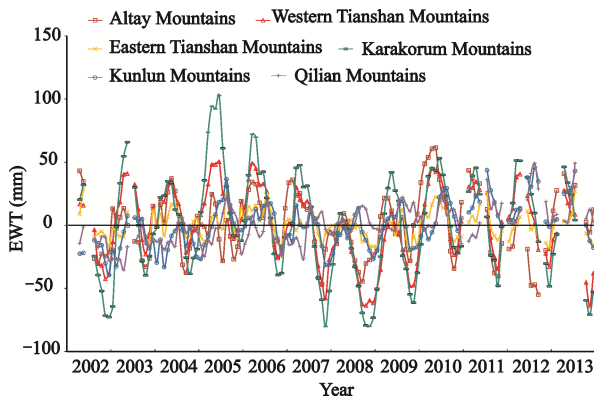


Fig. 6 Temporal variations in water storage changes in the six subzones

Based on the curves showing temporal changes, all of the temporal variations of water storage changes in the

six parts are cyclical. At the same time, the scale, amplitude and tendency of the six mountain ranges are different. To enable assessment of the characteristics of the yearly variations in water storage changes integrally, the cumulative EWT change among the subzones are compared (Fig. 7).

Fig. 7 shows the cumulative EWT changes among the six subzones over the entire study period. Based on the assessed quality of the data, the period extending from 2004 to 2010 was examined. The Karakorum Mountains, the Kunlun Mountains and the Western Tianshan Mountains display similar trends, the pattern seen in the Eastern Tianshan Mountains is similar to that of the Altay Mountains, and the pattern seen in the Qilian Mountains is opposite to that of the Eastern Tianshan Mountains and

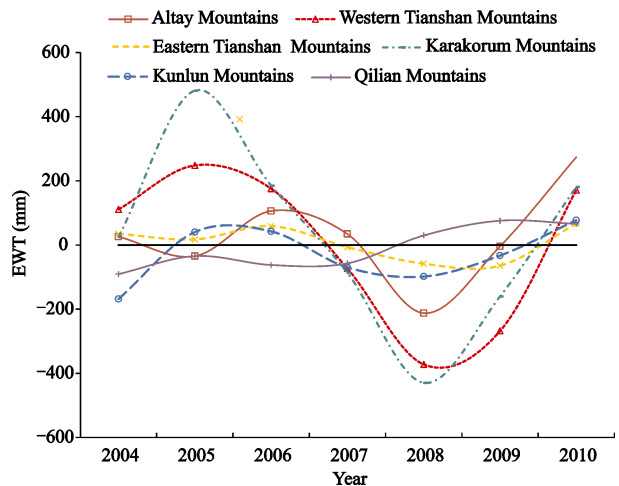


Fig. 7 Comparisons of the cumulative equivalent water thickness (EWT) changes among the subzones

the Altay Mountains. Moreover, the amplitudes are, from largest to smallest, Karakorum Mountains > Western Tianshan Mountains > Eastern Tianshan Mountains > Kunlun Mountains > Qilian Mountains. The amplitude in the Altay Mountains increased over time. The largest degree of dispersion seen in the six subzones is that of the Karakorum Mountains, and its standard deviation is 270.41, whereas the smallest is that of the Eastern Tianshan Mountains, which has a value of 48.78. Overall, the ordering of the degree of dispersion of the six subzones is Karakorum Mountains > Western Tianshan Mountains > Altay Mountains > Kunlun Mountains > Qilian Mountains > Eastern Tianshan Mountains. This sequence is largely in line with the monthly variations, and this result further confirms the effects of climate change.

3.1.3 Spatial variation of water storage change in different mountains

The graphs shown in Fig. 8 present comparisons between

pairs of adjacent mountain ranges (a and b) and comparisons in the north-south and west-east directions (c and d). The comparison of the changes in the six subzones presented in Fig. 8 indicates the temporal and spatial variations of water storage changes and reflects obvious intra-annual and interannual changes. Based on the characteristics of these distributions, we perform pairwise comparisons and compare the changes in the north-south and west-east directions.

Based on Fig. 8, the adjacent mountain ranges (the Eastern Tianshan Mountains and the Western Tianshan Mountains, as well as the Karakorum Mountains and the Kunlun Mountains) display similar trends; however, the Western Tianshan Mountains and the Karakorum Mountains display larger amplitudes than the Eastern Tianshan Mountains and the Kunlun Mountains, respectively. In addition, the latter mountain ranges display more volatility than the former ranges. Taken together,

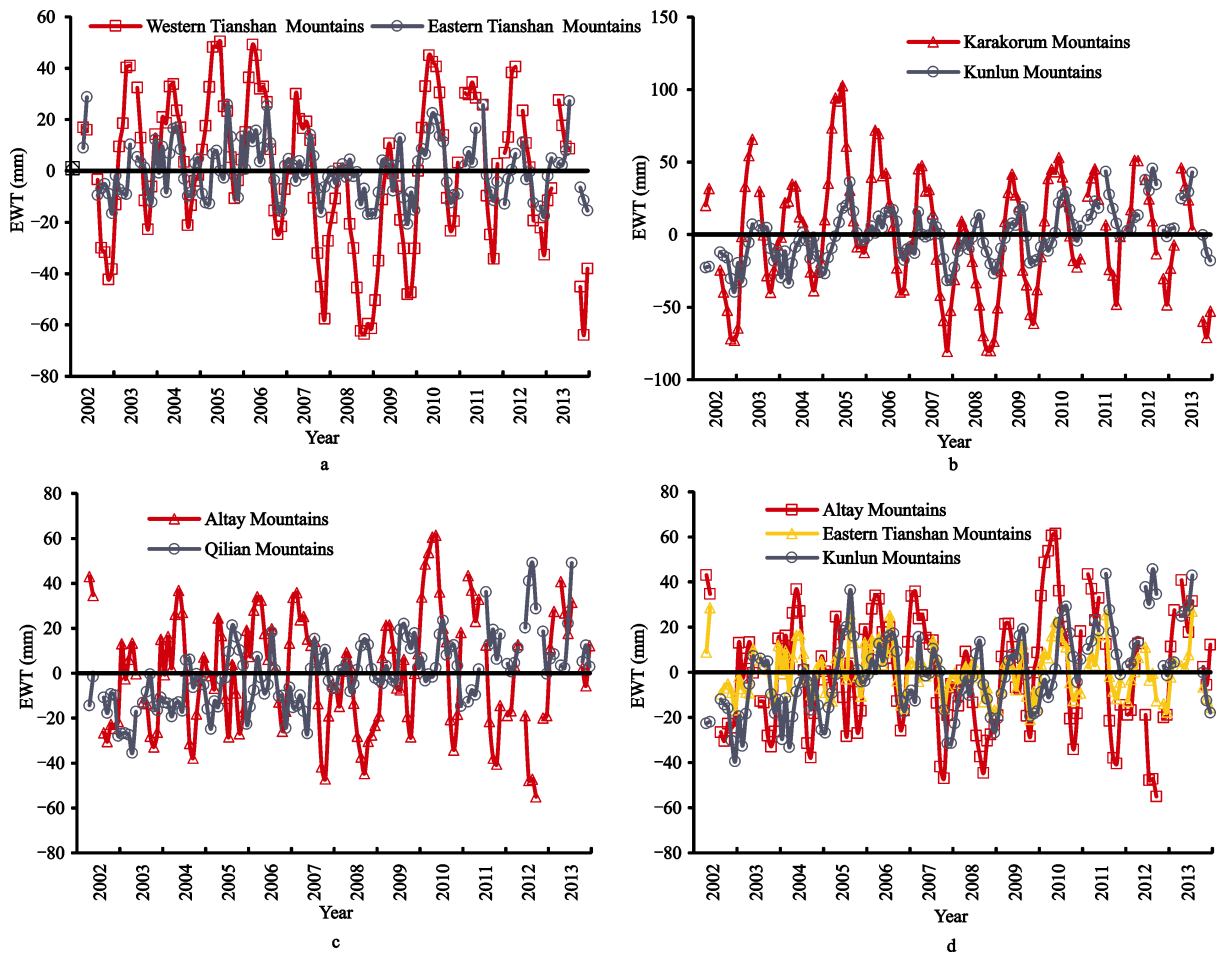


Fig. 8 Comparisons of equivalent water thickness (EWT) changes in the six subzones (a. Eastern Tianshan Mountains and Western Tianshan Mountains b. Karakorum Mountains and Kunlun Mountains c. Altay Mountains and Qilian Mountains d. Altay Mountains, Eastern Tianshan Mountains and Kunlun Mountains)

the water storage changes in these four mountain ranges all indicate increases from 2002 to 2005 and 2008 to 2010, and they reflect decreases from 2005 to 2008 and 2010 to 2013. Thus, the trends in these ranges are bimodal.

The Altay Mountains and the Qilian Mountains display opposite trends most of the time. However, a comparison of the EWT changes among the Altay Mountains, the Eastern Tianshan Mountains and the Kunlun Mountains shows no clear relationship among the three parts. On the other hand, the Altay Mountains display a more stable changing trend, with the exception of a larger peak in 2010. However, the EWT changes in the Qilian Mountains display a clear increase over time.

To further assess the degree of dispersion of the spatial variations in water storage in the different mountain ranges, the standard deviations of the EWT changes within each mountain range are calculated from April 2002 to December 2013. The largest degree of dispersion is that of the Karakorum Mountains, which has a value of 40.40, and the smallest is that of the Eastern Tianshan Mountains, with a value of 10.79. In descending order, the standard deviations of the six subzones are as follows: Karakorum Mountains > Western Tianshan Mountains > Altay Mountains > Kunlun Mountains > Qilian Mountains > Eastern Tianshan Mountains.

3.2 Influence of precipitation on total water storage

To analyze the relationships between the EWT changes and precipitation within the study area, the data representing the EWT changes and precipitation covering the same period are compared to identify the patterns of variation of these two variables (Fig. 9). Fig. 9 shows the comparisons between the EWT changes and precipitation within the subzones. As shown in Fig. 9, the precipitation characteristics of the six subzones correspond to those of temperate continental climates; annual precipitation is low and mainly concentrated in summer, little or no rain occurs during the other seasons, and there is occasional snowfall during the winter. The largest amounts of precipitation occurred during the period from June to August every year.

Considering all of the mountain ranges, the most positive EWT changes and precipitation amounts appear simultaneously, and some of the patterns reflect hysteresis behaviour. Based on Fig. 9, the connections between

precipitation and EWT changes are strongest in the Kunlun Mountains and the Qilian Mountains, followed by the Eastern Tianshan Mountains. The Karakorum Mountains and the Western Tianshan Mountains have poorer connections between these variables, whereas that of the Altay Mountains is the poorest. That is, the EWT changes of the Kunlun Mountains and the Qilian Mountains are strongly determined by precipitation, and the EWT changes of the Eastern Tianshan Mountains are affected by precipitation to some extent, whereas the EWT changes of the Karakorum Mountains and the Western Tianshan Mountains are apparently controlled by other hydrological factors.

In terms of the degree of dispersion of precipitation within the six subzones, the smallest is that of the Eastern Tianshan Mountains, regardless of whether the monthly mean values or those of whole study period are considered. The corresponding standard deviations are 12.57 and 14.32, respectively. The same conclusion applies to the degree of dispersion of the EWT changes. On the other hand, the largest value is that of the Qilian Mountains, which differs from the degree of dispersion of the EWT changes, which may be caused by other factors.

3.3 Influence of ice cover on total water storage

Ice cover is the other major factor that influences total water storage in the mountainous areas of Central Asia, especially in summer and winter. The changes in ice cover show a strong seasonal pattern.

To analyze the relationship between the EWT changes and snow cover within the six subzones, the data representing EWT changes and snow-covered area covering the same period are compared to find the patterns of variation of these two variables (Fig. 10).

As shown in Fig. 10 most of the local maxima in snow-covered area occur simultaneously with local minima of the EWT changes in the Karakorum Mountains and the Altay Mountains. On the other hand, in the Kunlun Mountains, the Eastern Tianshan Mountains and the Qilian Mountains, data values reflecting opposite extremes appear at the same time. Furthermore, the extreme values of total water storage appear to lag behind those of ice-covered area.

To compare the effects of precipitation and ice-covered area, the correlation coefficients between precipitation or snow-covered area and EWT changes are shown in Table 2.

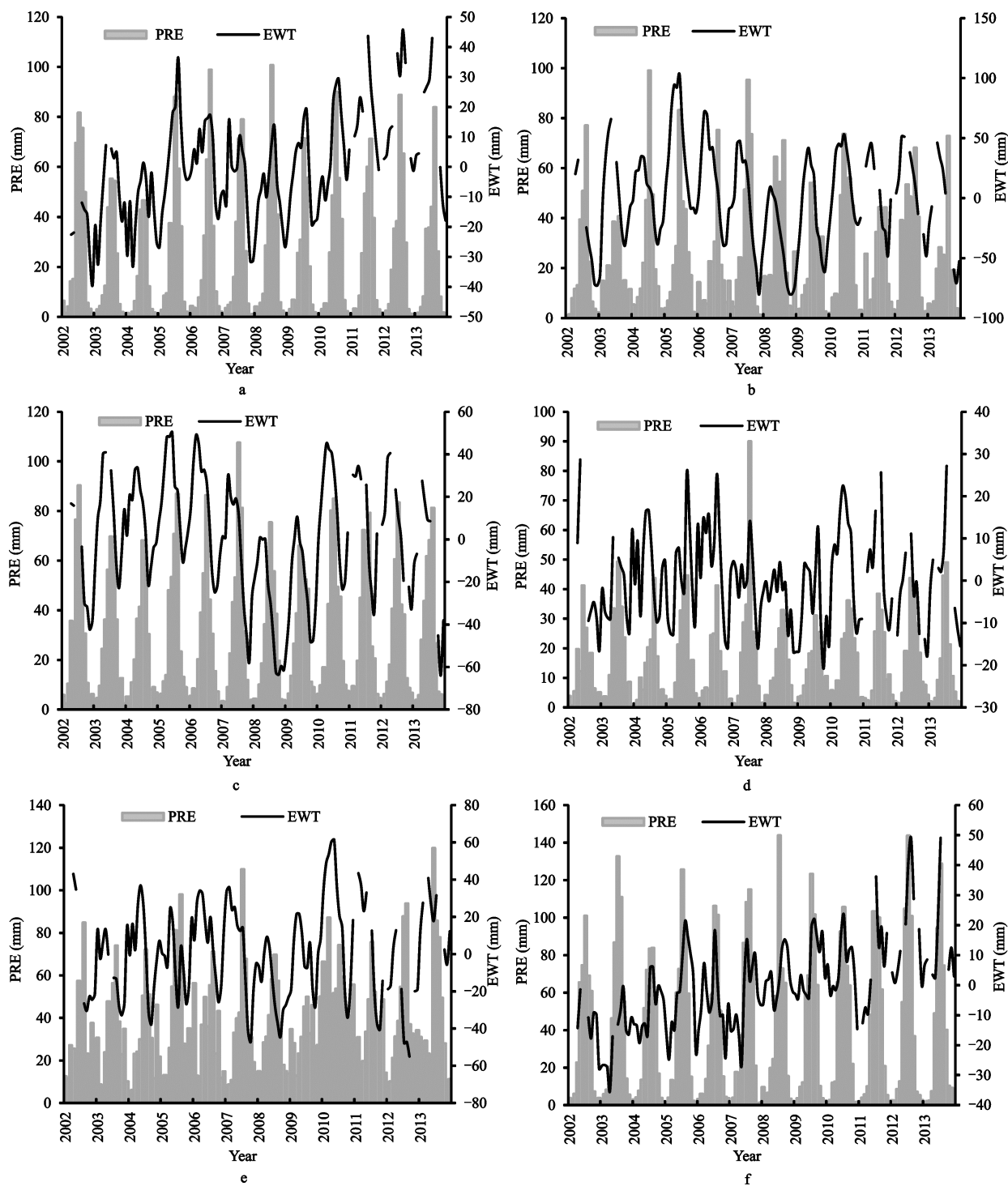


Fig. 9 Comparisons between equivalent water thickness (EWT) changes and precipitation (PRE) in the different subzones (a. Kunlun Mountains; b. Karakorum Mountains; c. Western Tianshan Mountains; d. Eastern Tianshan Mountains; e. Altay Mountains; f. Qilian Mountains; PRE (precipitation))

As shown in Table 2 the largest correlation coefficients between precipitation and total water storage among the six subzones correspond to the Kunlun Mountains and the Qilian Mountains, for which the

values are 0.591 and 0.490, respectively. The Eastern Tianshan Mountains takes second place, whereas the correlation coefficients associated with the Karakorum Mountains and the Western Tianshan Mountains are

smaller, and the correlation between precipitation and the EWT changes in the Altay Mountains is the lowest. In addition, except for the Altay Mountains, the results pass a test of significance at the 0.01 level.

Snow-covered area and EWT changes are negatively correlated in the Kunlun Mountains, the Qilian Mountains and the Eastern Tianshan Mountains, for which the values are -0.552 , -0.439 and -0.383 . In addition,

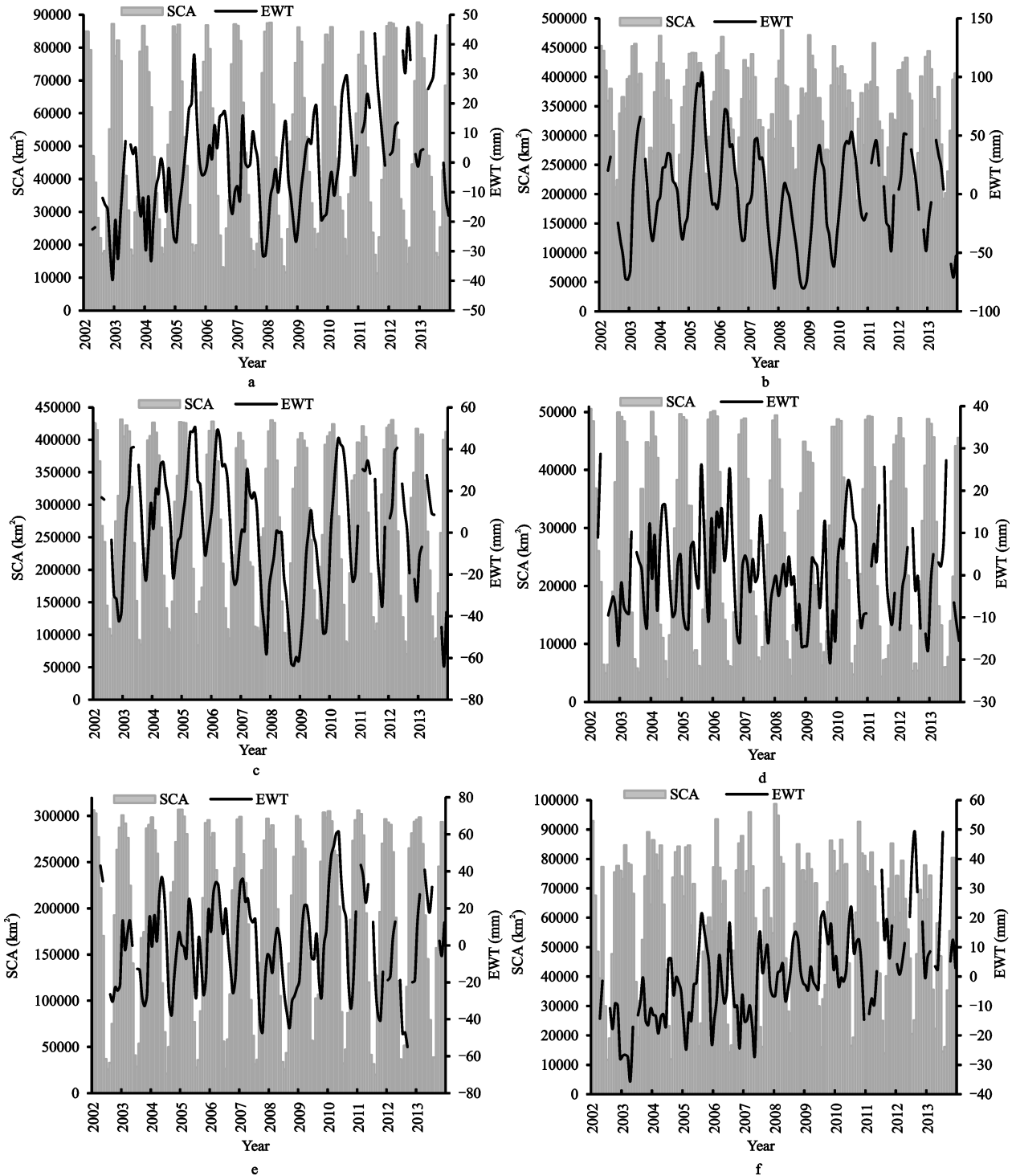


Fig. 10 Comparisons between equivalent water thickness changes and snow-covered area within subzones (a. Kunlun Mountains; b. Karakorum Mountains; c. Western Tianshan Mountains; d. Eastern Tianshan Mountains; e. Altay Mountains; f. Qilian Mountains SCA (snow-covered area))

Table 2 Correlation coefficients between precipitation (PRE) or snow-covered area (SCA) and equivalent water thickness changes

RANGE	PRE	SCA
Kunlun Mountains	0.591**	-0.552**
Karakorum Mountains	0.247**	0.042
Western Tianshan Mountains	0.268**	-0.168
Eastern Tianshan Mountains	0.426**	-0.383**
Altay Mountains	-0.045	0.178*
Qilian Mountains	0.490**	-0.439**

Notes: ** indicates statistical significance the significant test at the 0.01 level, * indicates statistical significance at the 0.05 level

the results pass a test of significance at the 0.01 level. The correlation coefficient associated with the Altay Mountains is positive, and the results pass a test of significance at the 0.05 level. On the other hand, the correlation coefficients between the snow-covered areas and the EWT changes of the Karakorum Mountains and the Western Tianshan Mountains are lower.

Comparing the correlations between precipitation and ice-covered area to EWT changes, except for the Altay Mountains, the correlation coefficients between precipitation and EWT change are larger than those for ice-covered area and EWT changes. Therefore, except for the Altay Mountains, precipitation is the major factor that drives water storage changes.

4 Discussion

4.1 Patterns of total water storage change in different mountain ranges

The effects of human activities are comparatively small in mountainous areas. Therefore, the most important factors that can influence water storage in mountainous areas are precipitation and meltwater from snow and ice. Xu *et al.* (2013) found that the overall amount of total water storage in the Tianshan Mountains is greater in the western and eastern parts of the range and less in the middle portion of the range. The increase in total water storage occurs because of the increased precipitation that occurs in summer. Furthermore, the decrease in water storage is due to climate warming, which has caused accelerated glacier retreat. The overall amount of total water storage in the Qilian Mountains is greater in the western and southern parts of the range and less in the eastern and northern parts of the range. The total water storage has increased from 2003 to 2010 in the Qilian Mountains because the climate warming has

melted the permafrost and caused the active layer to thicken (Xu *et al.*, 2014). Climate change is a factor that drives changes in total water storage, especially in high-altitude regions (Tangdamrongsub *et al.*, 2011). The results of these studies are the same as those presented in this article. Natural factors influence the changes in total water storage in the mountainous areas of Central Asia, and the changes in the different sub-zones are different because the different circulation patterns lead to different precipitation regimes and different changes in snow cover.

The Altay Mountains are influenced by westerly air flow. These air masses pass Lake Zaysan in Russia, follows the deep Irtysh River valley, and then rise because of the obstacle presented by the Altay Mountains. Finally, they cause additional precipitation. The precipitation gradually increases with the altitude. Moreover, the isohyet runs roughly northwest-southeast, and the amount of precipitation that falls is larger in summer and winter. The snow-covered area of the Altay Mountains is smallest in July and August; the snow begins to accumulate in October and increases greatly in November and December. The snow-covered area reaches its maximum in January. The snow-covered area then begins to go down in February and March and reaches a minimum in June.

The climate of the Tianshan Mountains can be divided into two parts that consist of a cool season and a warm season, and the precipitation and elevations decrease gradually from west to east. The northern slope of the Tianshan Mountains is influenced by air flow from the Atlantic Ocean and the Arctic Ocean, so the precipitation on the northern slope is greater than on the southern slope. The snow-covered area of the Tianshan Mountains begins to increase substantially in November, and it reaches a maximum in January. The snow-covered area begins to decrease at the end of March. It reaches its minimum at the end of May.

Because of its topography, the climate in the Karakorum Mountains is influenced by westerly winds, and precipitation is abundant in spring and winter. The southern slope is much moister than the northern slope because of monsoon precipitation from the Indian Ocean. On the other hand, the climate in the Kunlun Mountains is nearly unaffected by monsoon precipitation from the Indian and Pacific Oceans. In contrast, it is strongly influenced by continental air masses. The mid-

dle section of the Kunlun Mountains is much drier, whereas the western and eastern parts are relatively humid. Snow begins in October and persists through April of the following year, and the amount of snow deposited during this time accounts for more than 71% of the yearly snowfall. The snow-covered area displays strong seasonal fluctuations. From June to May of the following year, the snow-covered area reflects a normal distribution. The snow cap in the Kunlun Mountains appears in mid-August. The snow-covered area then becomes larger until the peak value appears in January. The snow-free season in the Kunlun Mountains is comparatively short and extends from March to August. Moreover, there are some areas of permanent snow cover, primarily within the Karakorum Mountains and the West Kunlun Mountains.

While the Qilian Mountains represent the transition zone between the desert region in the western and northern parts of China and the high, cold region of the Tibetan Plateau, it is far away from the ocean. The Qilian Mountains lies within the mid-latitude westerlies. Because of the uplift of the Qinghai-Xizang plateau, the westerlies were divided into two. In addition, the north branch is stronger, and the westerly jet blows parallel to the northern margin of the Qilian Mountains towards the east. The climate of the Qilian Mountains is mainly controlled by the westerly jet, which forms a pressure ridge, and the weather is dry and cold. In summer, the atmospheric circulation is more complex because the westerlies shift northwards. Both the southwest monsoon from Indian Ocean and the southeast monsoon from the Pacific Ocean affect this subzone. However, the Qilian Mountains lie in the hinterland of the Asian mainland, and they are surrounded by high mountains. Thus, the warm and wet air masses from the east and south reach their limits, so that they cause limited amounts of precipitation. The snow cover in the Qilian Mountains displays a two-peaked curve, as snowfall increases and temperatures decrease until December, when snow cover reaches its maximum value. Subsequently, snow cover reaches a minimum value at the end of December because of prolonged drought. In January, given the persistent rain and low temperatures, the snow cover in the Qilian Mountains grows even faster, and at the end of February it begins to decline.

Based on the different circulation patterns and their variations, the interannual and seasonal water storage

variations in the different subzones are different. Moreover, as global warming intensifies, hydrological extremes occur more frequently, and the total water storage of these subzones, which can easily be affected by precipitation, display greater variability. The details of the effects of precipitation and snow cover represent a problem that can be investigated in future work.

4.2 Influence of precipitation and ice cover on total water storage

The influence of precipitation on total water storage is different in the six subzones. The Kunlun Mountains and the Qilian Mountains are the most heavily affected by precipitation, and the maxima between precipitation and total water storage display hysteresis behaviour.

Sun Qian found that the maximum in water storage normally corresponds to the precipitation maximum with a certain time lag in Central Asia (Sun *et al.*, 2014). The results of this study are the same as those presented in this article. In mountainous areas, total water storage is mainly influenced by precipitation and snow cover, the maxima of precipitation in the mountainous areas of Central Asia appear in summer. The precipitation values increase from January to July or August, and the maxima often appear in July or August. After the summer, precipitation begins to decrease until the end of the year. Moreover, the amount of snowmelt in the six subzones also reaches its maximum in summer. The snow-covered area decreases from January to July or August, and the minimum value appears in July or August. After summer, the snow cover begins to increase until the end of the year. In fact, the total water storage in the mountainous areas of Central Asia is influenced by the difference between the amount of precipitation and the amount of snowmelt. Total water storage increases as the precipitation increases in the mountains; however, total water storage decreases with increasing snowmelt amount. However, the times at which precipitation and ice cover have the greatest effects on total water storage differ because of the different processes by which they influence total water storage.

Precipitation intensity and the buffering role of snowmelt reach different levels in the different mountain ranges. Therefore, the changes in total water storage change differ among the six subzones. Meanwhile, our analysis shows that snow-covered area and total water storage are negatively correlated in the Kunlun Moun-

tains, Eastern Tianshan Mountains and Qilian Mountains. This phenomenon is mainly due to snow melt. When the snow begins to melt, the meltwater percolates quickly into the soil. Thus, as the snow melts, the total water storage influenced by snowmelt does not change during the initial stages, while precipitation continues to increase and the total water storage increases, which is the reason for the observed negative correlation between snow-covered area and total water storage. In the meantime, the lags between the two factors (snow-covered area and precipitation) and total water storage is also due to the influence of these processes and the time over which they operate.

5 Conclusions

In the research, the spatial-temporal change pattern of water storage in Central Asia was studied and the influences of precipitation and snow-covered area were compared. Based on the above findings, considering the changes that occur within the four representative months, EWT changes in April and July reflect increases, whereas a EWT changes that reflect decreases were observed in November. Therefore, the total water storage in the mountainous regions of Central Asia increases in winter and summer, partly due to precipitation, although some parts display hysteresis behaviour. The annual spatial variability of the EWT change reflects movement of the area with positive values from west to east from January to December. Moreover, the EWT changes within the study area decreased from 2002 to 2004 and then returned to a higher level from 2005 to 2006; subsequently, the EWT changes remained at a lower level from 2007 to 2009, and after 2010, the EWT gradually increased. The temporal variations of water storage changes in the Mountainous areas of Central Asia are cyclical. In addition, the spatial variations of the water storage changes in a single year show that the area with positive values moves from west to east. The most positive EWT changes and precipitation amounts appear simultaneously, and some of the patterns reflect hysteresis behaviour. Precipitation has a stronger effect on water storage changes than snow-covered area in the mountainous regions of Central Asia.

The Altay Mountains have undergone the most pronounced changes. The trend in this region, is opposite

that of the Qilian Mountains. Meanwhile, the variability in EWT changes in the Altay Mountains has increased over time, although the closeness of the relationship between these values and precipitation is the least strong of any of the mountain ranges. Thus, the EWT changes within the Altay Mountains have become increasingly variable over time and display a strong resistance to precipitation forcing, which leads us to the conclusion that snow-cover area and other factors acting upon the Altay Mountains. The Western Tianshan Mountains and the Eastern Tianshan Mountains display similar trends in EWT changes because of their proximity. However, the EWT changes in the Eastern Tianshan Mountains display sharper peaks than those of the Western Tianshan Mountains, and the amplitude of the EWT changes is larger for the Western Tianshan Mountains than the Eastern Tianshan Mountains. The EWT changes in the Eastern Tianshan Mountains are more strongly affected by precipitation than those of the Western Tianshan Mountains. The Karakorum Mountains and the Kunlun Mountains also display similar trends because of their proximity. The amplitude of EWT changes in the Karakorum Mountains is bigger than that of the Kunlun Mountains, and the proximity of the Kunlun Mountains is larger than that of the Karakorum Mountains. The total water storage change of the two ranges is less affected by precipitation. The Qilian Mountains displays the most obvious increase in EWT changes over time and the smallest amplitude changes. Meanwhile, the total water storage in the Qilian Mountains is affected by precipitation to a much greater degree than the other parts.

References

- Andersen O B, Hinderer J, 2005. Global inter-annual gravity changes from grace: early results. *Geophysical Research Letters*, 32(1): L01402. doi: 10.1029/2004GL020948
- Baker R H A, Sansford C E, Jarvis C H *et al.*, 2000. The role of climatic mapping in predicting the potential geographical distribution of non-indigenous pests under current and future climates. *Agriculture, Ecosystems & Environment*, 82(1-3): 57-71. doi: 10.1016/S0167-8809(00)00216-4
- Crowley J W, Mitrovica J X, Bailey R C *et al.*, 2008. Annual variations in water storage and precipitation in the Amazon Basin. *Journal of Geodesy*, 82(1): 9-13. doi: 10.1007/s00190-007-0153-1
- Chen J L, Wilson C R, Seo K W, 2006. Spatial sensitivity of the gravity recovery and climate experiment (GRACE) time-variable gravity observations. *Journal of Geophysical*

- Research*, 111(B6): B08408. doi: 10.1029/2005JB004064
- Güntner A, 2008. Improvement of global hydrological models using GRACE data. *Surveys in Geophysics*, 29(4-5):375-397. doi: 10.1007/s10712-008-9038-y
- Hu X G, Chen J L, Zhou Y H et al., 2006. Seasonal water storage change of the Yangtze River basin detected by GRACE. *Science in China Series D*, 49(5): 483–491. doi: 10.1007/s11430-006-0483-5
- Lemoine J M, Bruinsma S, Loyer S, et al., 2007. Temporal gravity field models inferred from GRACE data. *Advances in Space Research*, 39(10):1620-1629. doi: 10.1016/j.asr.2007.03.062
- Nastula J, Salstein D A, Popiński W, 2015. Hydrological excitations of polar motion from GRACE gravity field solutions. In: Rizos C, Willis P. *IAG 150 Years. International Association of Geodesy Symposia*. Cham: Springer, 513–519. doi: 10.1007/1345_2015_85
- Rodell M, Famiglietti J S, 2001. An analysis of terrestrial water storage variations in Illinois with implications for the Gravity Recovery and Climate Experiment (GRACE). *Water Resources Research*, 37(5):1327–1339. doi: 10.1029/2000WR900306
- Rodell M, Houser P R, Jambor U et al., 2004. The global land data assimilation system. *Bulletin of the American Meteorological Society*, 85(3): 381–394. doi: 10.1175/BAMS-85-3-381
- Rodell M, Velicogna I, Famiglietti J S, 2009. Satellite-based estimates of groundwater depletion in India. *Nature*, 460(7258): 999–1002. doi: 10.1038/nature08238
- Seyoum W M, Milewski A M, 2016. Monitoring and comparison of terrestrial water storage changes in the northern high plains using GRACE and in-situ based integrated hydrologic model estimates. *Advances in Water Resources*, 94: 31–44. doi: 10.1016/j.advwatres.2016.04.014
- Seyoum W M, Milewski A M, 2016. Monitoring and comparison of terrestrial water storage changes in the northern high plains using GRACE and in-situ based integrated hydrologic model estimates. *Advances in Water Resources*, 94: 31–44. doi: 10.1016/j.advwatres.2016.04.014
- Shi Yafeng, Shen Yongping, Hu Ruji, 2002. Preliminary study on signal, impact and foreground of climatic shift from warm-dry to warm-humid in northwest China. *Journal of Glaciology and Geocryology*, 24(3): 219–226. doi: 10.3969/j.issn.1000-0240.2002.03.001 (in Chinese)
- Sun Guiyan, Guo Lingpeng, Chang Cun et al., 2006. Contrast and analysis of water storage changes in the north slopes and south slopes of the central Tianshan Mountains in Xinjiang. *Arid Land Geography*, 39(2): 254–264. doi: 10.13826/j.cnki.cn65-1103/x.2016.02.004 (in Chinese)
- Sun Qian, Tashpolat T, Ding Jianli et al., 2014. GRACE data-based estimation of spatial variations in water storage over the central Asia during 2003-2013. *Acta Astronomica Sinica*, 55(6): 498–511. (in Chinese)
- Swenson S, Wahr J, 2002. Methods for inferring regional surface-mass anomalies from Gravity Recovery and Climate Experiment (GRACE) measurements of time-variable gravity. *Journal of Geophysical Research*, 107(B9): 2193. doi: 10.1029/2001JB000576
- Swenson S, Wahr J, Milly P C D, 2003. Estimated accuracies of regional water storage variations inferred from the Gravity Recovery and Climate Experiment (GRACE). *Water Resources Research*, 39(8): 1223. doi: 10.1029/2002WR001808
- Tangdamrongsub N, Hwang C, Kao Y C, 2011. Water storage loss in central and south Asia from GRACE satellite gravity: correlations with climate data. *Natural Hazards*, 59(2):749-769. doi: 10.1007/s11069-011-9793-9
- Tapley B D, Bettadpur S, Watkins M, et al., 2004. The gravity recovery and climate experiment: Mission overview and early results. *Geophysical Research Letters*, 31(31):4 PP. doi: 10.1029/2004GL019779
- Wahr J, Molenaar M, Bryan F, 1998. Time variability of the Earth's gravity field: hydrological and oceanic effects and their possible detection using GRACE. *Journal of Geophysical Research*, 103(B12): 30205–30229. doi: 10.1029/98JB02844
- Wahr J, Swenson S, Zlotnicki V et al., 2004. Time-variable gravity from GRACE: first results. *Geophysical Research Letters*, 31(11): L11501. doi: 10.1029/2004GL019779
- Wang Puyu, Li Zhongqin, Wang Wenbin et al., 2014. Glacier volume calculation from ice-thickness data for mountain glaciers—a case study of glacier No. 4 of Sigong River over Mt. Bogda, Eastern Tianshan, Central Asia. *Journal of Earth Science*, 25(2): 371–378. doi: 10.1007/s12583-014-0427-5
- Xu Min, Ye Baisheng, Zhao Qiudong et al., 2013. Spatiotemporal Change Of Water Reserves in the Tianshan Mountains, Xinjiang Based on GRACE. *Arid Zone Research*, 30(3): 404–411. doi: 10.13866/j.azr.2013.03.003 (in Chinese)
- Xu Min, Zhang Shiqiang, Wang Jian et al., 2014. Temporal and spatial patterns of water storage change of Qilian Mountains in recent 8 years based on GRACE. *Arid Land Geography*, 37(3): 458–467. doi: 10.13826/j.cnki.cn65-1103/x.2014.03.006 (in Chinese)
- Yamamoto K, Fukuda Y, Nakaegawa T et al., 2007. Landwater variation in four major river basins of the Indochina peninsula as revealed by GRACE. *Earth, Planets and Space*, 59(4): 193–200. doi: 10.1186/BF03353095
- Yu Y T, Yang T B, Li J J et al., 2006. Millennial-scale Holocene climate variability in the NW China drylands and links to the tropical Pacific and the North Atlantic. *Palaeogeography, Palaeoclimatology, Palaeoecology*, 233(1–2): 149–162. doi: 10.1016/j.palaeo.2005.09.008
- Zhang Guanghui, Liu Shaoyu, Zhang Cuiyun et al., 2004. Evolution of groundwater circulation in the Heihe River drainage area. *Chinese Geology*, 31(3): 289–293. doi: 10.3969/j.issn.1000-3657.2004.03.008 (in Chinese)
- Zhang Z Z, Chao B F, Chen J L et al., 2015. Terrestrial water storage anomalies of Yangtze River Basin droughts observed by GRACE and connections with ENSO. *Global and Planetary Change*, 126: 35–45. doi: 10.1016/j.gloplacha.2015.01.002